

Supporting Information

Revealing Oxygen Reduction Reaction Activity Origin of Single Atom Supported on g-C₃N₄ Monolayer: A First-Principles Study

Huan Niu^a, Xiting Wang^a, Chen Shao^a, Yuanshuang Liu^b, Zhaofu Zhang^{c,*}, and
Yuzheng Guo^{a,*}

^a School of Electrical Engineering, Wuhan University, Wuhan, Hubei 430072, China

^b State Key Laboratory of Tribology, School of Mechanical Engineering, Tsinghua University, Beijing, 10084, China

^c Department of Engineering, Cambridge University, Cambridge, CB2 1PZ, United Kingdom

*To whom correspondence should be addressed. zz389@cam.ac.uk;
yguo@whu.edu.cn.

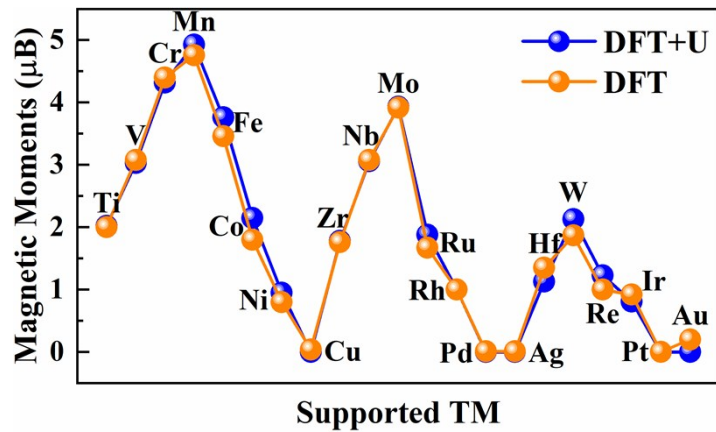


Figure S1. Magnetic moments of TM/g-C₃N₄ by applying DFT+U (Hubbard U-J=3 eV) compared with DFT method.

Table S1. The adsorption energies of OOH, O, and OH on Pd/g-C₃N₄ and Ag/g-C₃N₄ with DFT+U and DFT, respectively.

	Pd/g-C ₃ N ₄		Ag/g-C ₃ N ₄	
	DFT+U	DFT	DFT+U	DFT
ΔE* _{OOH} /eV	3.38	3.41	3.65	3.54
ΔE* _O /eV	2.55	2.48	3.05	2.98
ΔE* _{OH} /eV	0.39	0.41	0.33	0.27

Table S2. Calculated zero point energies (ZPE) and entropy of different adsorption species and gas molecules with unit eV. T=298.15 K.

	ZPE (eV)	TS (eV)
*OOH	0.44	0.00
*O	0.07	0.00
*OH	0.34	0.00
H ₂ O	0.58	0.67
H ₂	0.27	0.41

ZPE was defined as $ZPE = \sum_i \frac{1}{2}h\nu_i$, where i was the frequency number, ν_i was the frequency with unit cm⁻¹. the adsorbed species were only taken vibrational entropy (S_v) into account, as shown in the following formula:

$$S_v = \sum_i R \left\{ \frac{h\nu_i}{k_B T} \left[\exp\left(\frac{h\nu_i}{k_B T}\right) - 1 \right]^{-1} - \ln \left[1 - \exp\left(-\frac{h\nu_i}{k_B T}\right) \right] \right\}$$

among which $R = 8.314 \text{ J}\cdot\text{mol}^{-1}\cdot\text{K}^{-1}$, $T = 298.15 \text{ K}$, $h = 6.63 \times 10^{-34} \text{ J}\cdot\text{s}$, $k_B = 1.38 \times 10^{-23} \text{ J}\cdot\text{K}^{-1}$, where i was the frequency number, ν_i was the frequency with unit cm⁻¹. The entropies of H₂O, H₂ can be obtained from the NIST database⁽¹⁾ with standard condition.

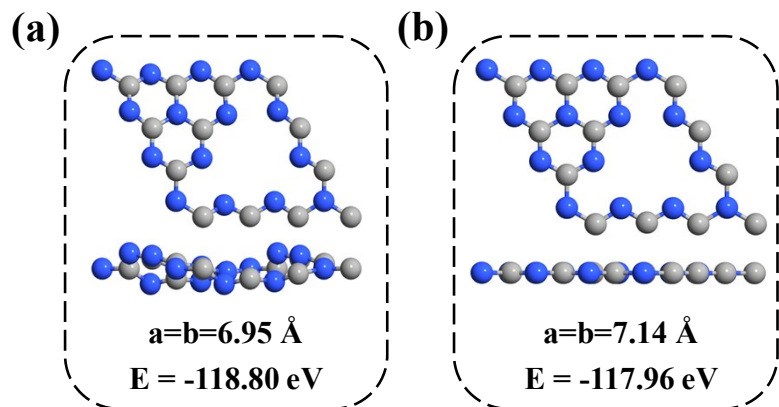


Figure S2. Top view and side view of (a) buckle and (b) planar $\text{g-C}_3\text{N}_4$, respectively. The lattice constant and total energy are listed.

The buckle $\text{g-C}_3\text{N}_4$ model is employed with a lattice constant of 6.95 \AA , in good agreement with previous study.¹ Compared with the planar $\text{g-C}_3\text{N}_4$ model, the lattice constant of the buckle one is also close to the experimental observation (6.81 \AA).² Moreover, the buckle $\text{g-C}_3\text{N}_4$ model processes more negative total energy (-0.84 eV per C_6N_8 cell) than the planar one. Thus, these results demonstrate the reasonable theoretical model is applied in this work.

Table S3. The bond length between TM atom and neighboring N atoms ($d_{\text{TM-N}}$) with unit Å. The deviation degree (ε) between TM atom and the center of cavity. The average bond length between TM and N atoms(d_{ave}) with unit Å.

	$d_{\text{TM-N}}$					
Ti	2.23	2.23	2.30	2.45	2.47	2.31
V	2.32	2.32	2.30	2.30	2.31	2.31
Cr	2.47	2.52	2.20	2.26	2.44	2.40
Mn	2.31	2.37	2.36	2.30	2.54	2.33
Fe	2.53	2.62	2.17	2.16	2.36	2.46
Co	2.73	2.63	1.94	1.95	2.61	2.76
Ni	2.77	2.52	1.91	1.92	2.72	2.82
Cu	2.16	2.31	2.17	2.50	2.84	2.56
Zr	2.28	2.28	2.31	2.41	2.42	2.31
Nb	2.31	2.32	2.31	2.31	2.32	2.31
Mo	2.49	2.42	2.08	2.19	2.85	2.78
Ru	2.85	3.38	2.89	2.08	2.03	2.03
Rh	2.91	3.35	2.77	2.10	2.04	2.13
Pd	3.01	3.16	2.41	2.26	2.44	2.40
Ag	2.33	2.71	2.55	2.33	2.71	2.60
Hf	2.31	2.41	2.40	2.31	2.25	2.25
W	2.24	2.43	2.21	2.37	2.21	2.41
Re	2.62	3.06	2.96	2.39	1.95	1.78
Ir	2.84	3.31	2.91	2.07	2.03	2.03
Pt	2.92	3.13	2.51	2.25	2.48	2.25
Au	2.31	2.78	2.62	2.32	2.77	2.66

Table S4. The diffusion energy barriers of Mn, Mo, Ru, W, Re and Ir and Pt from one cavity of g-C₃N₄ to another.

	Mn	Mo	Ru	W	Re	Ir	Pt
E _{barriers} /eV	2.48	2.67	2.11	3.50	2.54	2.30	1.93

Table S5. Binding energies of single and dimer TM for Mn, Mo, Ru, W, Re, Ir and Pt/g-C₃N₄.

	Mn	Mo	Ru	W	Re	Ir	Pt
ΔE _{bind} /eV	-2.96	-3.22	-3.63	-4.27	-3.24	-3.47	-2.67
ΔE _{bind2} /eV	-2.19	-2.70	-2.83	-3.77	-2.69	-3.06	-1.52

To confirm the stability of single TM supported on g-C₃N₄, binding energy of dimer TM (per TM) is calculated by

$$\Delta E_{bind2} = (E_{TM\ 2/g-C_3N_4} - E_{g-C_3N_4} - 2E_{TM-single}) / 2$$

where $E_{TM\ 2/g-C_3N_4}$, $E_{g-C_3N_4}$ and $E_{TM-single}$ are the total energy of g-C₃N₄ (with and without TM dimer) and single TM atom, respectively. Compared with ΔE_{bind2} , ΔE_{bind} values are more negative for Mn, Mo, Ru, W, Re, Ir and Pt/g-C₃N₄. Thus, single TM atoms supported on g-C₃N₄ are reasonably stable owing to the difficult formation of dimer TM.

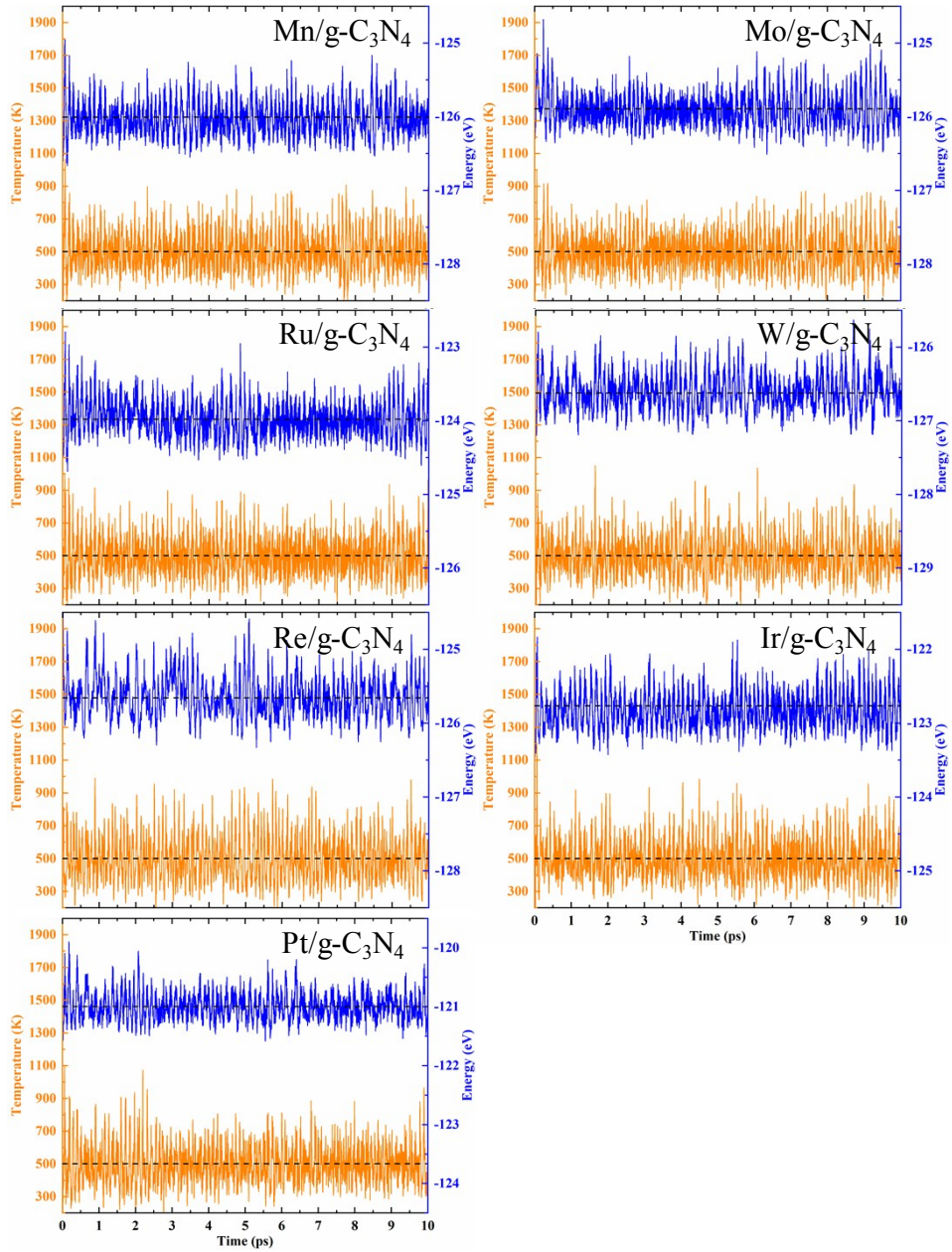


Figure S3. Variations of energy and temperature versus the AIMD simulation time for Mn, Mo, Ru, W, Re, Ir and Pt/g-C₃N₄, the simulation lasts for 10 ps at 500 K.

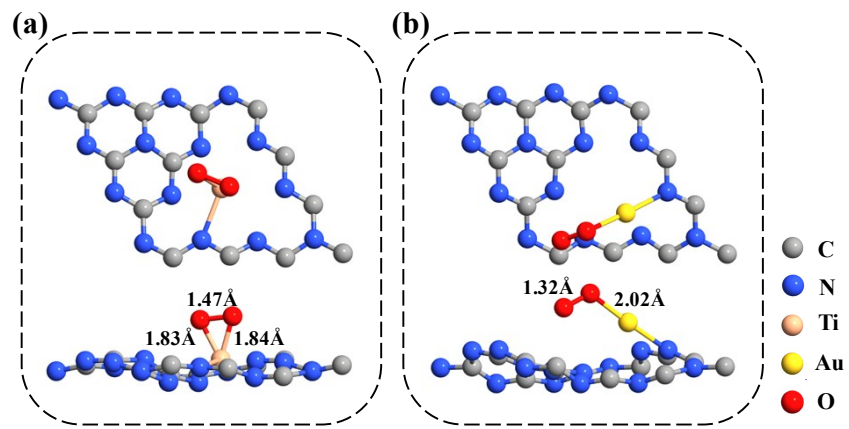


Figure S4. (a) The side-on configuration of O₂ adsorbed on Ti/g-C₃N₄. (b) the end-on configuration of O₂ adsorbed on Au/g-C₃N₄. The length of TM-O bonds and O-O bonds are shown in the figure.

Table S6. The adsorption energies and bond lengths of O₂ on TM/g-C₃N₄.

	$\Delta E^*_{O_2}/\text{eV}$	$d_{\text{TM-O1}}/\text{\AA}$	$d_{\text{TM-O2}}/\text{\AA}$	$d_{\text{O-O}}/\text{\AA}$
Ti	-3.77	1.83	1.84	1.47
V	-2.95	1.80	1.84	1.45
Cr	-2.35	1.79	1.86	1.44
Mn	-2.22	1.82	1.82	1.44
Fe	-1.87	1.88	1.92	1.41
Co	-2.55	1.79	1.79	1.38
Ni	-2.25	1.81	1.81	1.37
Cu	-0.97	1.84	/	1.33
Zr	-4.56	1.96	1.96	1.50
Nb	-3.47	1.94	1.92	1.47
Mo	-2.94	1.93	1.93	1.46
Ru	-1.87	1.88	2.01	1.40
Rh	-1.96	1.98	2.02	1.34
Pd	-1.18	1.99	2.01	1.36
Ag	-0.46	2.14	/	1.32
Hf	-4.80	1.94	1.95	1.52
W	-3.39	1.92	1.94	1.49
Re	-3.33	1.93	1.93	1.48
Ir	-2.48	1.96	2.00	1.38
Pt	-1.85	1.93	2.01	1.43
Au	-1.39	2.02	/	1.32

* O₂ molecule prefers to a kind of end-on adsorption on Cu, Ag, and Au/g-C₃N₄.

Table S7. The adsorption energies and bond lengths of OOH on TM/g-C₃N₄.

	$\Delta E^*_{\text{OOH}}/\text{eV}$	$d_{\text{TM-O}}/\text{\AA}$		$d_{\text{O-O}}/\text{\AA}$	$d_{\text{O-H}}/\text{\AA}$
Ti	-2.61	1.63	1.88	/	0.97
V	-1.96	1.60	1.80	/	0.97
Cr	2.65		1.87	1.48	0.98
Mn	2.55		1.92	1.48	0.98
Fe	2.64		1.84	1.51	0.98
Co	2.68		1.80	1.50	0.98
Ni	2.83		1.76	1.48	0.98
Cu	2.94		1.81	1.49	0.98
Zr	-2.86	1.76	2.02	/	0.97
Nb	-2.06	1.70	1.95	/	0.97
Mo	-2.22	1.69	1.92	/	0.98
Ru	2.59		1.72	1.56	0.98
Rh	2.77		1.90	1.45	0.99
Pd	3.41		1.97	1.45	0.99
Ag	3.54		2.08	1.48	0.98
Hf	-3.00	1.77	2.00	/	0.97
W	-2.24	1.72	1.95	/	0.97
Re	-2.13	1.71	1.90	/	0.97
Ir	2.12		1.86	1.49	0.98
Pt	2.93		1.93	1.46	0.98
Au	2.81		2.04	1.49	0.98

* OOH becomes O and OH absorbed on Ti, V, Zr, Nb, Mo, Hf, W and Re/g-C₃N₄.

Table S8. The adsorption energies and bond lengths of O on TM/g-C₃N₄.

	$\Delta E^*_O/\text{eV}$	$d_{\text{TM-O}}/\text{\AA}$
Ti	-2.10	1.62
V	-0.87	1.59
Cr	0.41	1.61
Mn	0.92	1.65
Fe	0.76	1.69
Co	0.93	1.65
Ni	1.49	1.66
Cu	2.21	1.73
Zr	-2.63	1.76
Nb	-1.65	1.70
Mo	-1.30	1.68
Ru	0.53	1.68
Rh	1.39	1.72
Pd	2.48	1.84
Ag	2.98	2.00
Hf	-2.76	1.76
W	-1.71	1.71
Re	-1.20	1.72
Ir	0.09	1.73
Pt	1.30	1.78
Au	1.73	1.88

Table S9. The adsorption energies and bond lengths of OH on TM/g-C₃N₄.

	$\Delta E_{\text{OH}}/\text{eV}$	$d_{\text{TM-O}}/\text{\AA}$	$d_{\text{O-H}}/\text{\AA}$
Ti	-1.55	1.85	0.98
V	-0.82	1.84	0.98
Cr	-0.70	1.83	0.97
Mn	-0.73	1.89	0.97
Fe	-0.63	1.83	0.97
Co	-0.59	1.78	0.97
Ni	-0.28	1.80	0.97
Cu	-0.36	1.80	0.97
Zr	-2.02	1.94	0.97
Nb	-0.97	1.97	0.98
Mo	-1.09	1.91	0.98
Ru	-0.55	1.89	0.99
Rh	-0.34	1.89	0.99
Pd	0.41	1.99	0.97
Ag	0.27	2.05	0.97
Hf	-2.30	1.92	0.97
W	-1.16	1.95	0.97
Re	-1.33	1.92	0.97
Ir	-1.02	1.88	0.98
Pt	-0.23	1.93	0.98
Au	-0.30	1.97	0.97

Table S10. The adsorption energies and bond lengths of H₂O on TM/g-C₃N₄.

	$\Delta E_{*H_2O}/\text{eV}$	$d_{\text{TM-O}}/\text{\AA}$	$d_{\text{O-H1}}/\text{\AA}$	$d_{\text{O-H2}}/\text{\AA}$
Ti	-0.61	2.21	0.98	1.01
V	-0.46	2.16	0.97	1.02
Cr	-0.43	2.43	0.97	0.99
Mn	-0.67	2.26	0.97	0.98
Fe	-0.76	2.14	0.97	1.02
Co	-0.97	2.01	0.97	1.03
Ni	-1.35	1.95	0.98	1.03
Cu	-0.69	2.07	0.98	1.02
Zr	-0.54	2.39	0.98	0.98
Nb	-0.20	/	0.97	0.98
Mo	-0.81	2.24	0.97	1.04
Ru	-0.40	/	0.97	0.98
Rh	-0.36	/	0.97	0.98
Pd	-0.66	2.31	0.97	1.01
Ag	-0.45	2.55	0.97	1.00
Hf	-0.76	2.23	0.97	1.05
W	-0.33	/	0.97	1.00
Re	-1.52	2.15	0.97	1.09
Ir	-0.41	/	0.97	0.98
Pt	-0.96	2.20	0.97	1.02
Au	-1.01	2.07	0.97	1.07

*H₂O absorbs on TM atoms with hydrogen bond for Nb, Ru, Rh, W and Ir/g-C₃N₄.

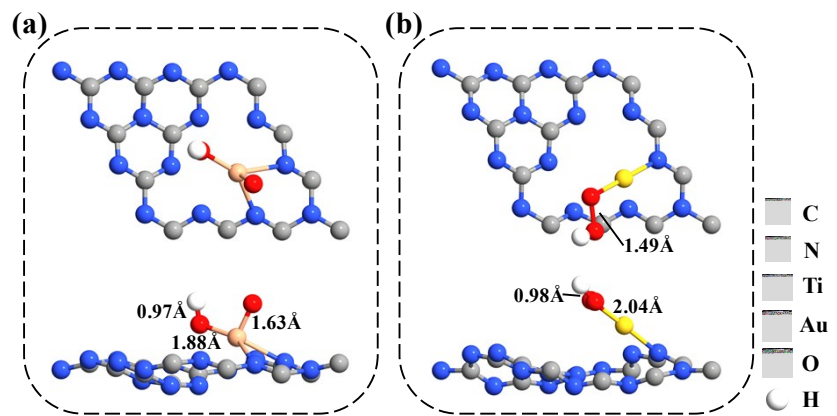


Figure S5. The configurations of (a) the dissociated OOH adsorbed on Ti/g-C₃N₄ and (b) the undissociated OOH adsorbed on Au/g-C₃N₄. The length of TM-O bonds, O-O bonds and O-H bonds are shown in the figure.

Table S11. The adsorption energies of OOH, O, and OH on Pd/g-C₃N₄ with a 2 × 2 × 1 supercell compared with a unit cell.

Pd/g-C ₃ N ₄	2 × 2 × 1	1 × 1 × 1
ΔE* _{OOH} /eV	3.49	3.41
ΔE* _O /eV	2.54	2.48
ΔE* _{OH} /eV	0.44	0.41

Table S12. ORR free energy changes of every step on TM/C₃N₄ with unit eV. (U is set to be 0 V)

	ΔG ₁	ΔG ₂	ΔG ₃	ΔG ₄
Ti	-7.12	0.13	0.89	1.19
V	-6.47	0.70	0.39	0.46
Cr	-1.86	-2.63	-0.77	0.34
Mn	-1.96	-2.02	-1.31	0.37
Fe	-1.87	-2.27	-1.05	0.27
Co	-1.83	-2.14	-1.18	0.23
Ni	-1.68	-1.73	-1.43	-0.08
Cu	-1.57	-1.12	-2.23	0.00
Zr	-7.37	-0.16	0.95	1.66
Nb	-6.57	0.02	1.02	0.61
Mo	-6.73	0.53	0.55	0.73
Ru	-1.92	-2.45	-0.73	0.19
Rh	-1.74	-1.77	-1.39	-0.02
Pd	-1.10	-1.32	-1.73	-0.77
Ag	-0.97	-0.95	-2.37	-0.63
Hf	-7.51	-0.15	0.80	1.94
W	-6.75	0.14	0.89	0.80
Re	-6.64	0.54	0.21	0.97
Ir	-2.39	-2.42	-0.77	0.66
Pt	-1.58	-2.02	-1.19	-0.13
Au	-1.70	-1.47	-1.69	-0.01

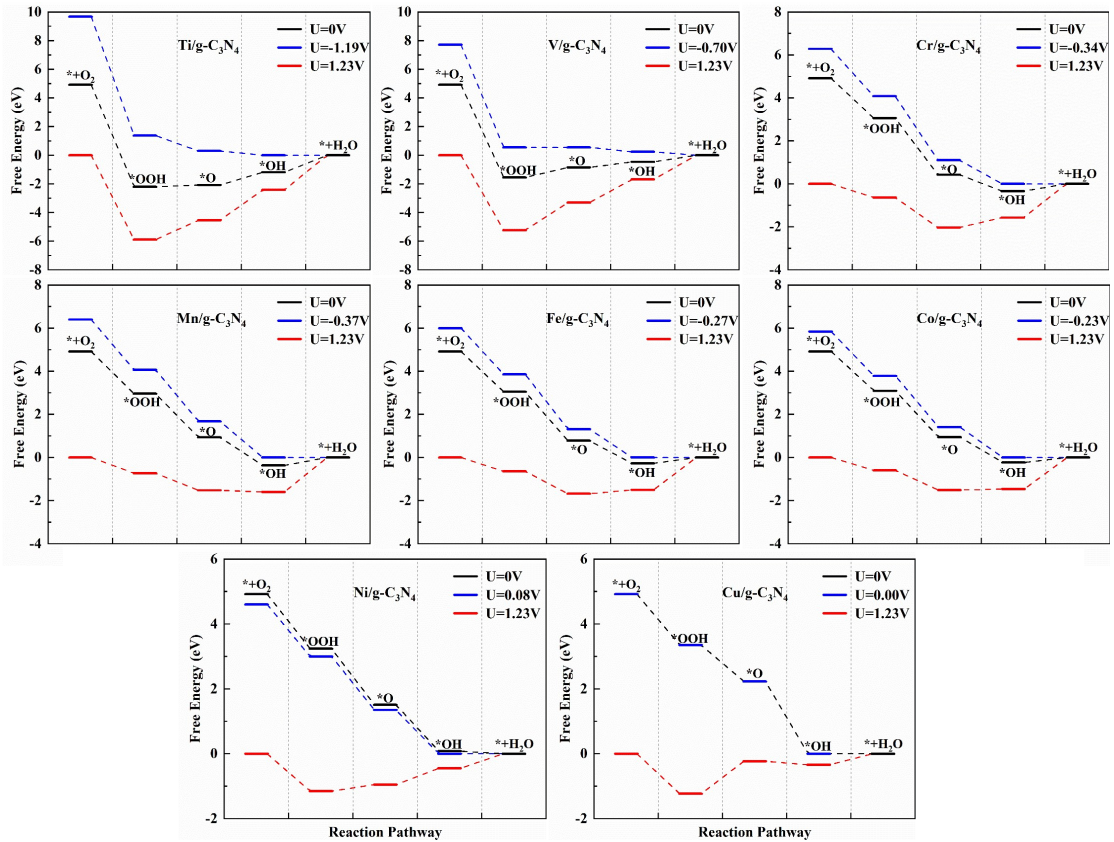


Figure S6. The ORR free energy diagrams of 3d TM atoms (TM=Ti, V, Cr, Mn, Fe, Co, Ni and Cu) supported on $\text{g-C}_3\text{N}_4$.

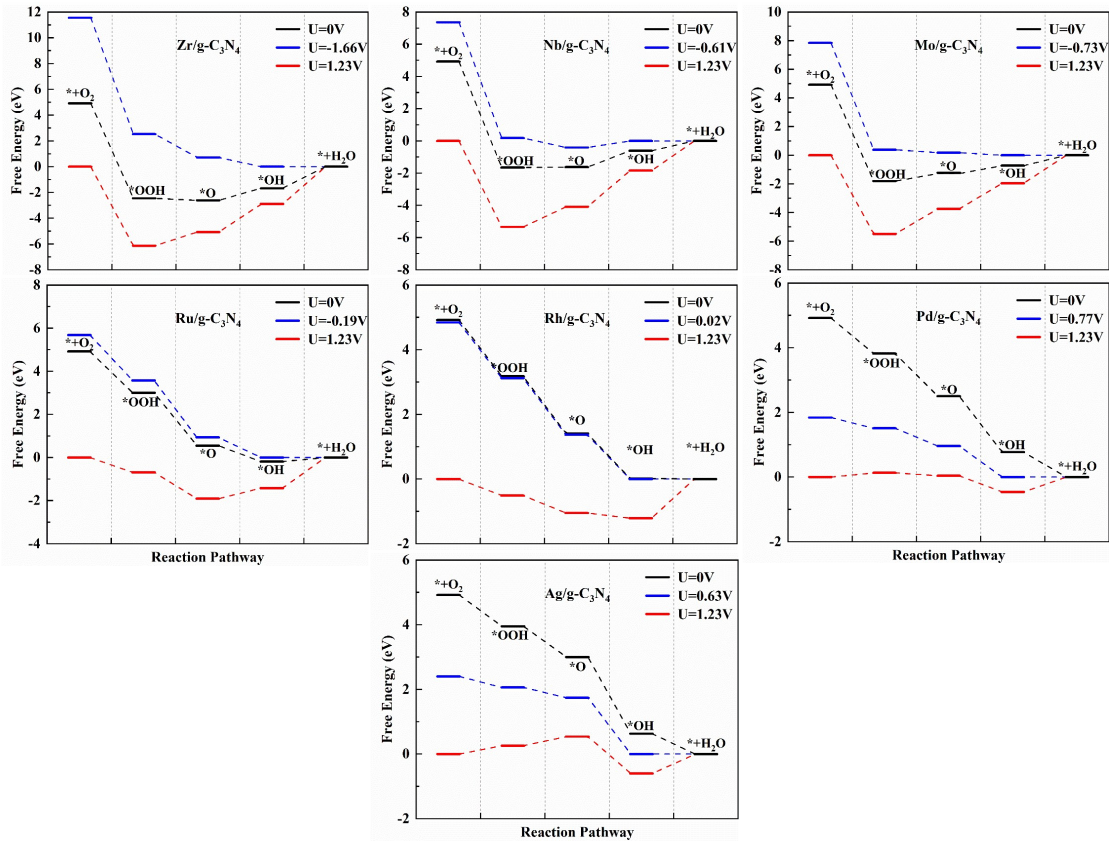


Figure S7. The ORR free energy diagrams of 4d TM atoms (TM=Zr, Nb, Mo, Ru, Rh, Pd and Ag) supported on $\text{g-C}_3\text{N}_4$.

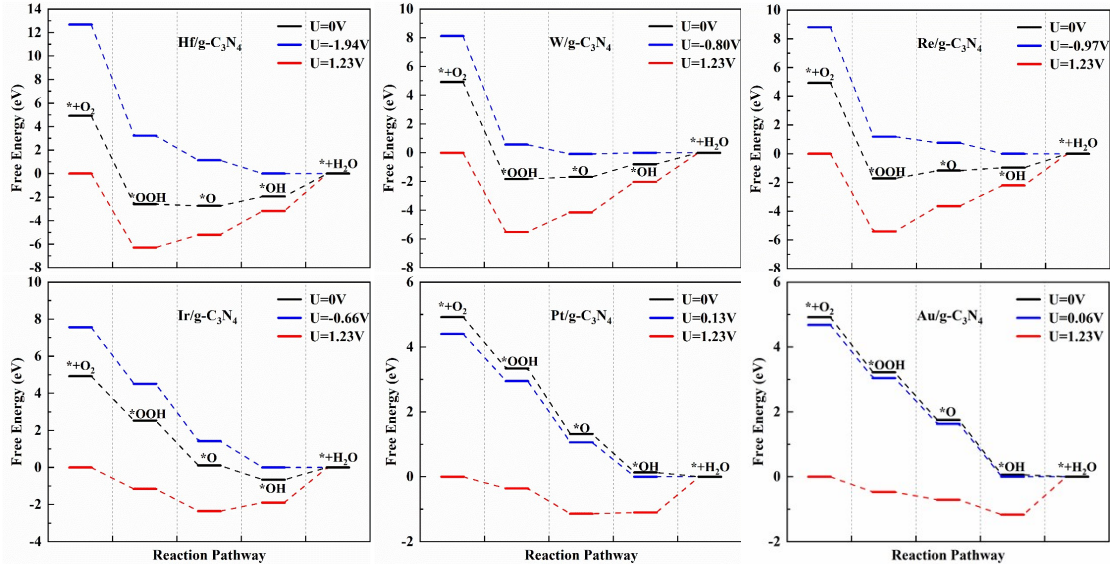


Figure S8. The ORR free energy diagrams of TM atoms (TM=Nb, Mo, Ru, Rh, Pd, Ag, Hf, W, Re, Ir, Pt and Au) supported on $\text{g-C}_3\text{N}_4$.

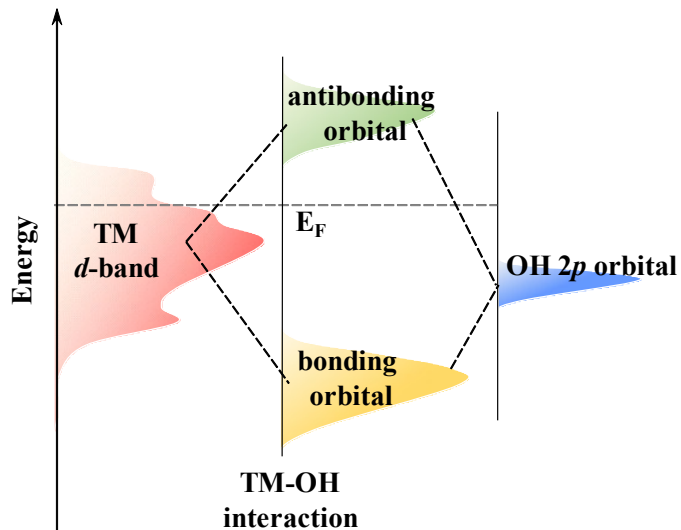


Figure S9. The schematic diagram illustrating how metal atom interact with OH on TM/g-C₃N₄, E_F denotes the Fermi level.

The electronic states of the metal atom interact with OH intermediate and their hybridized energy levels split into two groups. One is the bonding states that are generally occupied below E_F, and the other is the anti-bonding orbital that lies above E_F.

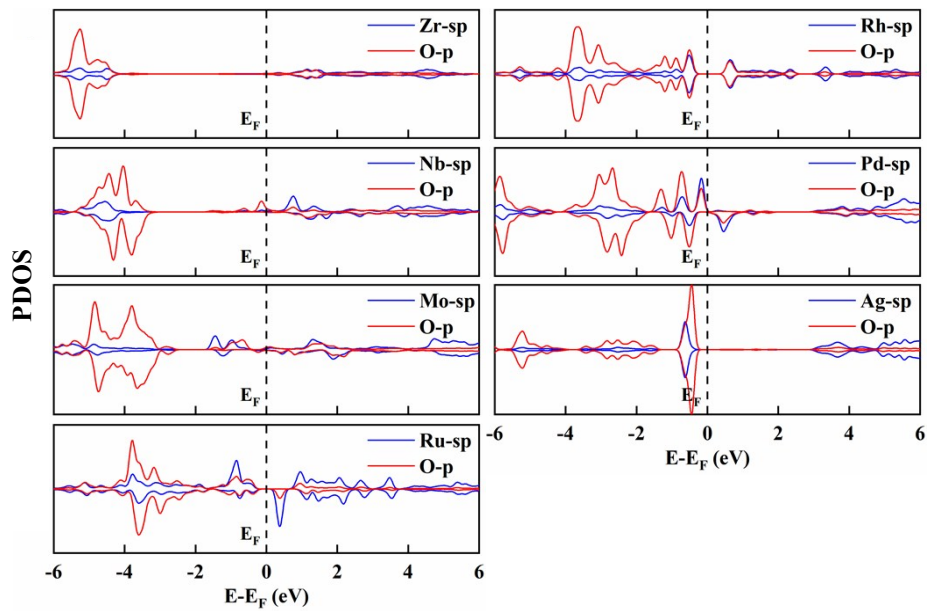


Figure S10. Partial density of 4d TM-sp orbitals and O-p orbitals on $g\text{-C}_3\text{N}_4$, E_F denotes the Fermi level and is set to zero.

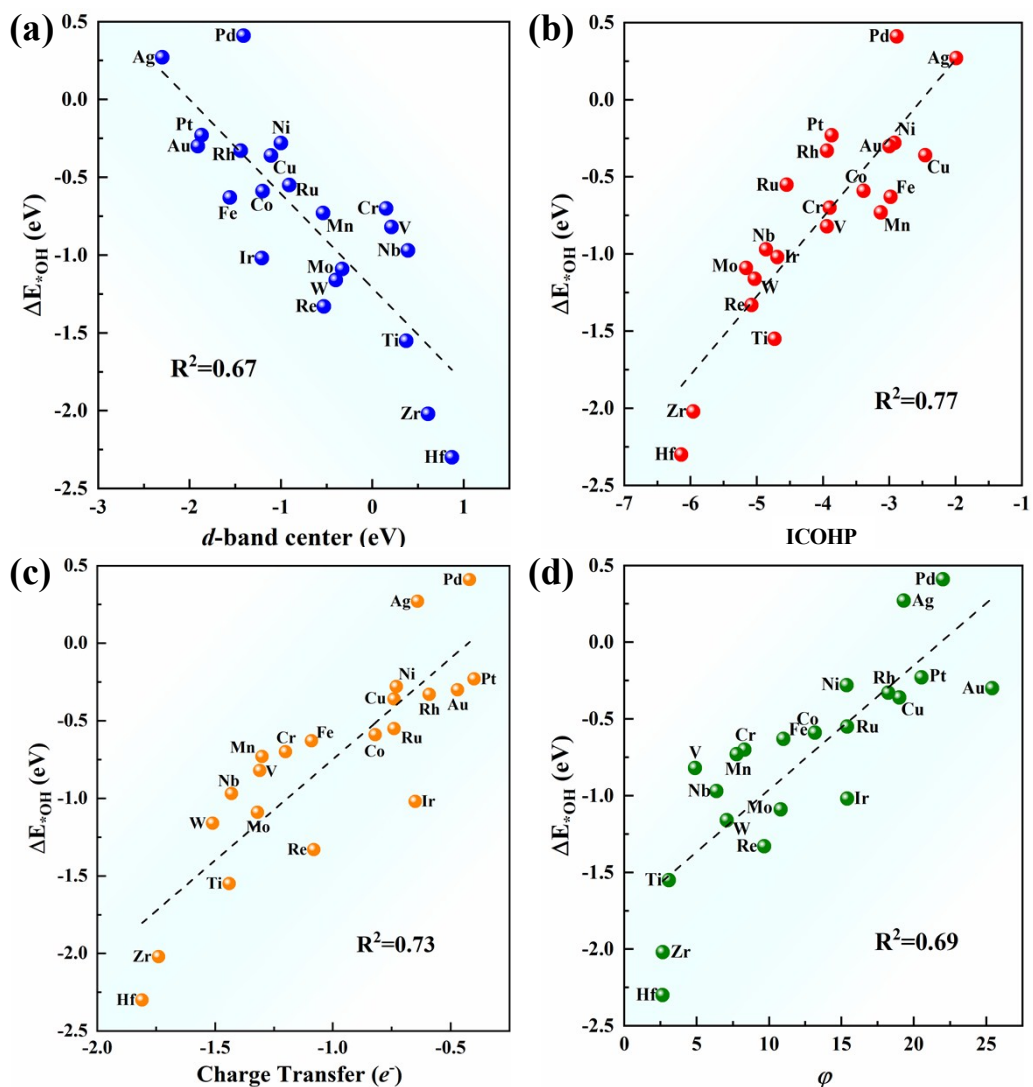


Figure S11. The linear relationships of ΔE_{*OH} versus d -band center, ICOHP, charge transfer as well as φ .

References

- 1 Computational Chemistry Comparison and Benchmark Database. <http://cccbdb.nist.gov/>.
- 2 Q. Gao, S. L. Hu, Y. Du and Z. P. Hu, *J. Mater. Chem. A*, 2017, **5**, 4827-4834.
- 3 X. Wang, K. Maeda, A. Thomas, K. Takanabe, G. Xin, J. M. Carlsson, K. Domen and M. Antonietti, *Nat. Mater.*, 2009, **8**, 76–80.